Development of a Radionuclide Inventory Evaluation Framework for a Soluble-Boron-Free SMR

Seungnam Lee, Woo Jin Lee, Ser Gi Hong *
[a] *Department of Nuclear Engineering, Hanyang University, 222 Wangsimni-ro, Seongdong-gu, Seoul, 04763*
**Corresponding author: hongsergi@hanyang.ac.kr*

Keywords : i-SMR, Source term, Radionuclide inventory, Soluble-boron-free, Control rod operation

1. Introduction

The innovative Small Modular Reactor (i-SMR) is a 170 MWe PWR-based SMR under development in Korea [1]. It adopts soluble-boron-free (SBF) operation through the use of advanced burnable absorbers and control rod insertion during normal operation. Control rod insertion changes the local power, neutron spectrum, and reaction rates. Therefore, the control rod position and operation history can affect the local radionuclide composition.

The core radionuclide inventory is a major component of the reactor source term for accident analyses [2]. A conventional simplified approach applies a core-average power and burnup history to a single ORIGEN calculation [3]. Although this approach efficiently estimates the whole-core inventory, it cannot directly represent the different operating histories over fuel assemblies, axial nodes, and fuel rods, and it also cannot reflect local power and neutron spectrum changes caused by control rod insertion.

In this study, a coupled reactor physics and radionuclide inventory evaluation framework was developed and applied to the first-cycle core of the i-SMR. Whole-core and local inventories calculated using the coupled DeCART2D/MASTER–Polaris/ORIGEN framework were compared with those from the conventional single ORIGEN calculation and an independent Serpent 2 depletion calculation as the reference. For a selected node in a control-rod-affected region, the effect of CR-operation history dependent ORIGEN libraries was also evaluated in detail.

2. Computational Methods and Models

2.1 i-SMR Core Model

The i-SMR core has a thermal power of 520 MWth and consists of 69 fuel assemblies with a 17 x 17 square lattice. It is designed for a 24-month cycle with a two-batch fuel management scheme. HIGA (Highly Intensive and Discrete Gadolinia/Alumina Burnable Absorber) and IGD (integral gadolinia) burnable absorbers are used to control excess reactivity under soluble-boron-free conditions [4]. Four regulating control rod banks (RB) are used during normal operation to maintain criticality.

Fig. 1 and 2 show the fuel assembly configurations and the core loading and control rod patterns used in this work, respectively. Eight fuel assembly types were designed, and their detailed compositions were summarized in Table I. Each fuel assembly contained 16 HIGA rods with varying the number of IGD rods. Fig. 2 shows the core loading and control rod patterns of the i-SMR. The control rods were organized into four regulating bank groups (R1, R2, R3, and R4) and one shutdown bank group (SB). Ag-In-Cd is used as the absorber material for the regulating banks, whereas B_4C enriched to 95% in ^{10}B is used for the shutdown bank.

Table I: Compositions of fuel assembly types.

Type	Fuel rod	HIGA	1st IGD			2nd IGD		
	^{235}U (wt.%)	Gd_2O_3 (mol.%)	^{235}U (wt.%)	GD wt.%	No.	^{235}U (wt.%)	GD wt.%	No.
A01	4.00	10	-	-	-	-	-	-
A02	4.00	10	3.50	4	4	-	-	-
A03	4.00	12	3.50	4	4	-	-	-
A04	4.00	14	3.50	4	4	2.50	8	4
A05	4.00	15	3.50	4	4	2.50	8	4
A06	4.00	16	3.50	4	4	2.50	8	4
A07	4.00	18	3.95	1	4	2.50	8	8
A08	4.00	18	3.75	2	4	2.50	8	8

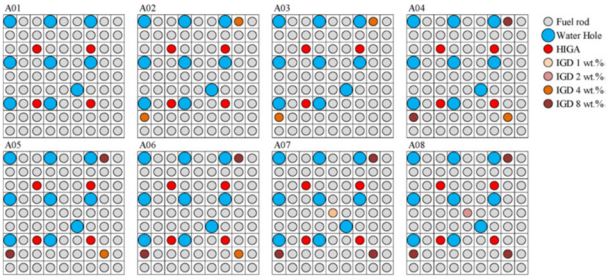


Fig. 1. Configurations of fuel assembly types for the i-SMR core.

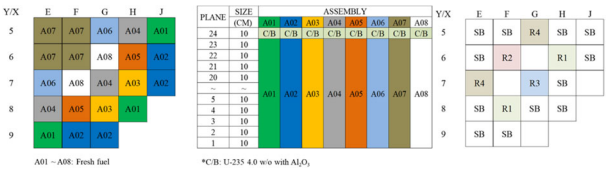


Fig. 2. Core loading and control rod patterns for the i-SMR core

2.2 Coupled Framework for Radionuclides' Inventory Evaluation

The DeCART2D/MASTER two-step reactor physics code system was developed by KAERI [5,6]. DeCART2D is 2-D MOC lattice code that generates homogenized two-group constants and heterogeneity

form functions. MASTER performs three-dimensional nodal depletion calculations, searches critical control rod positions, and reconstructs pin power distributions.

Polaris in the SCALE code system is a 2-D MOC lattice code using the Embedded Self Shielding Method (ESSM) for resonance treatment and it can generate ORIGEN libraries for different fuel assembly types, burnup conditions, and control rod states [7].

In this work, a computational framework is developed by combining the DeCART2D/MASTER code system and the Polaris/ORIGEN code system for detailed evaluation of radionuclides' inventories. The coupling of these codes was done using Python. In this framework, the ORIGEN cross section libraries were generated by Polaris considering node- or fuel rod-wise power histories. The node- or fuel rod-wise power histories for the ORIGEN calculations were evaluated using DeCART2D/MASTER code system. So, the ORIGEN calculations for source term were performed over the fuel rods or fuel assemblies. The mapping framework is shown in Fig. 3.

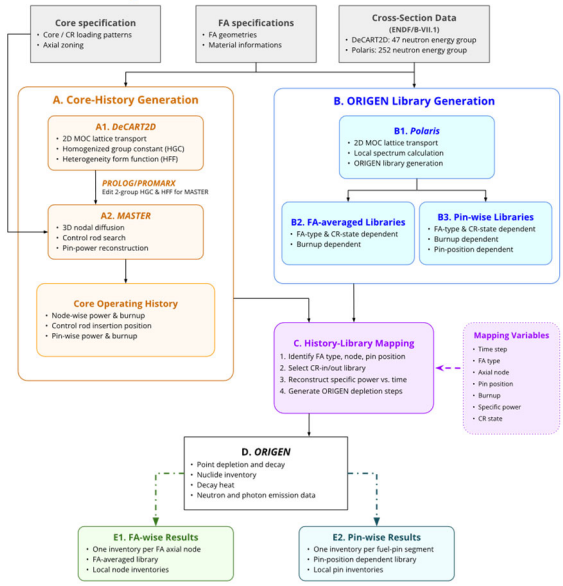


Fig. 3. Radionuclide inventory evaluation framework.

In this paper, three approaches were compared: 1) Single ORIGEN using the core-average history, 2) Node-wise ORIGEN using fuel assembly radial and axial segment histories, and 3) Pin-wise ORIGEN using fuel pin radial and axial segment histories.

2.3 Serpent 2 Reference Calculation

Serpent 2 is a continuous-energy Monte Carlo neutron transport and depletion code developed by VTT Technical Research Centre of Finland [8]. Each UO_2 fuel pellet and burnable absorber pellet were divided into three and eight equal-volume radial depletion zones, respectively, and the active core was divided into 24 axial zones. The control rod positions for criticality at each depletion step were adopted from the MASTER calculation. The detailed inventories calculated using Serpent 2 were used as the reference.

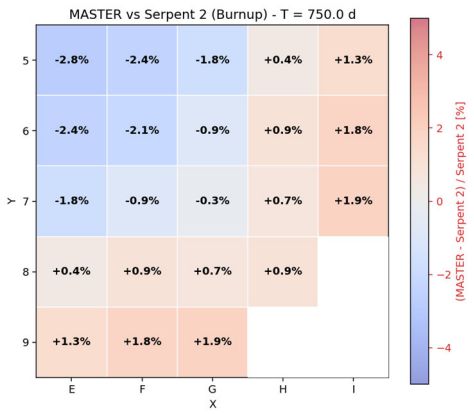
3. Results

3.1 Whole-core Inventory Comparison

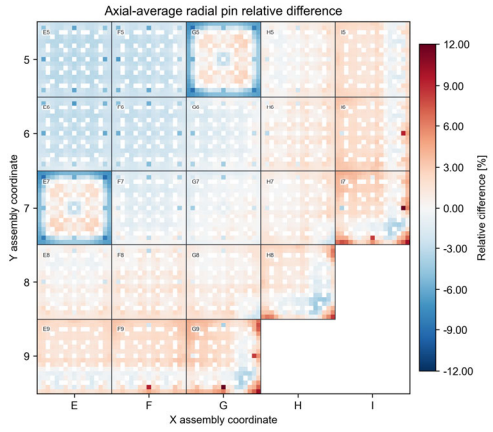
Table I summarizes the whole-core inventory results at EOC (End-of-Cycle). For the sum of the nine radionuclide groups, the relative differences of the single ORIGEN, node-wise ORIGEN, and pin-wise ORIGEN calculations with respect to Serpent 2 were 0.99%, 0.59%, and 0.71%, respectively. The corresponding mean absolute relative differences for the nine groups were 2.13%, 1.02%, and 1.12%, respectively.

The absolute relative difference for the noble metal group decreased from 3.69% in the single ORIGEN calculation to 0.03% and 0.40% in the node-wise and pin-wise calculations, respectively. In particular, it should be noted that the conventional single ORIGEN calculation less-conservatively underestimated the noble gases and halogens inventories by 0.53% and 5.06%, respectively. Table II also shows that the coupled framework calculations gave more accurate inventories than the conventional single ORIGEN calculation, except for the noble gases and lanthanides groups, for which the differences remained comparable.

Although the pin-wise calculation used a finer spatial resolution, it did not provide the most accurate results. This may be because it is difficult to accurately estimate the pin-wise burnup in the nodal diffusion code with pin power reconstruction method under the boron-free operation where the control insertion is used for reactivity control. Fig. 4 compares the axially-averaged radial burnup difference distributions obtained from MASTER and Serpent 2. At the assembly level, the absolute relative differences were within 3% for all assemblies. However, the pin-wise results showed a maximum absolute relative difference of 12.2%, and relatively large differences were observed in control rod affected assemblies such as E7 and G5. These differences may have affected the accuracy of the pin-wise ORIGEN calculation.



(a) Assembly-wise



(b) Pin-wise

Fig. 4. Comparison of axially-averaged radial burnup relative differences between MASTER and Serpent 2: (a) assembly-wise and (b) pin-wise.

3.2 Local Inventory in a Control Rod Insertion Region

Node E7-z16 shown in Fig. 5 was selected because it is located in the upper region of assembly E7, where the RB4 regulating control rod was repeatedly inserted during normal operation.

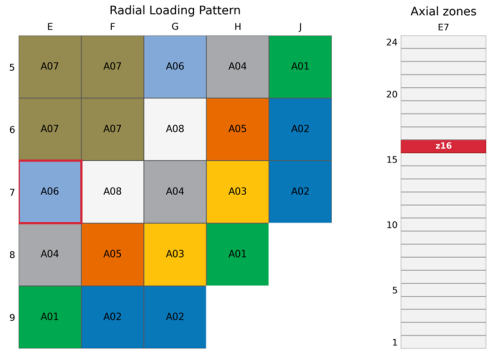
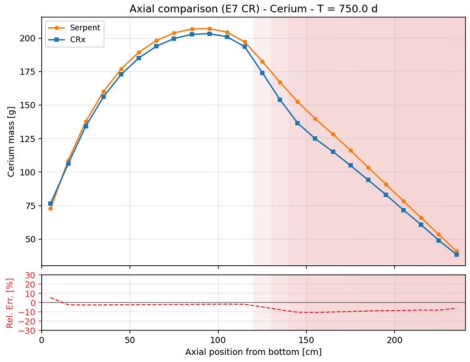
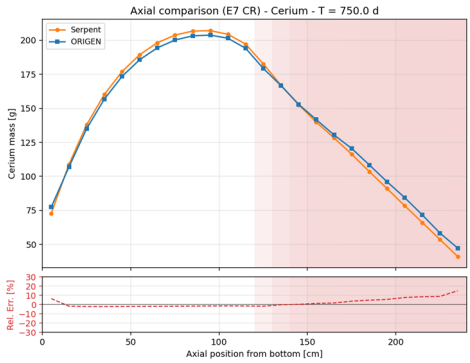


Fig. 5. Selected node E7-z16 for comparing local inventory calculations.

For assembly E7, Fig. 6 compares the axial cerium group inventory distributions at EOC. The cerium group was selected for comparison because it exhibited the largest inventory change due to control rod insertion. When the CR-operation history dependent libraries were selected according to the control rod operation history, the ORIGEN calculation gave a cerium group inventory distribution that closely agreed with the Serpent 2 result, and the assembly-integrated cerium group inventory was 0.19% higher than the reference. In contrast, when only the CR-out library was used throughout the irradiation history, the cerium group inventory was substantially underestimated by 4.44% relative to the reference.



(a) CR-out library only



(b) CR-operation history dependent libraries

Fig. 6. Axial cerium group inventory distributions obtained with (a) the CR-out library only and (b) CR-operation history dependent libraries.

Table III summarizes the inventories and relative differences for node E7-z16. The absolute relative difference in the total inventory and the mean absolute relative difference were reduced from 5.14% and 3.19% to 0.46% and 1.10%, respectively. The absolute relative differences for the Cerium Group, Noble Metals, and Halogens were reduced from 10.64%, 4.27%, and 6.95% to 1.32%, 0.32%, and 3.40%, respectively. These results indicate that control-rod induced local spectral changes should be considered to avoid unconservative inventory calculation in the rodded regions.

4. Conclusions

A coupled reactor physics and radionuclide inventory evaluation framework was applied to the first-cycle of the i-SMR core and compared against an independent Serpent 2 Monte Carlo calculation.

The coupled framework calculations reduced the mean absolute relative difference for the nine radionuclide groups from 2.13% for the conventional single ORIGEN calculation to 1.02% - 1.12%. For the individual radionuclide groups, the node-wise framework calculation was more accurate than the single ORIGEN calculation. However, the pin-wise calculation was less accurate for the noble gases and lanthanides groups than the single ORIGEN calculation. This may be because it is difficult to represent the effect of control rod insertion using pin power reconstruction.

For the selected control rod affected node, the use of CR-operation history dependent libraries reduced the absolute relative difference in the total inventory from 5.14% to 0.46%. In particular, the cerium group inventory showed an underestimation of 10.64% with the CR-out library, whereas the use of the CR-operation history dependent libraries reduced the difference to 1.32%. Therefore, both spatial operating histories and spectral changes caused by control rod insertion should be considered in radionuclide inventory evaluations for soluble-boron-free SMRs.

REFERENCES

[1] H.O. Kang, B.J. Lee, S.G. Lim, Light water SMR development status in Korea, Nuclear Engineering and Design 419 (2024) 112966. https://doi.org/10.1016/j.nucengdes.2024.112966.

[2] U.S. NRC, Accident source terms for light-water nuclear power plants, NUREG/CR (United States, Nucl. Reful. Comm.) 1465 (1995).

[3] M.J. Bell, ORIGEN: the ORNL isotope generation and depletion code, Oak Ridge National Lab., Tenn.(USA), 1973. https://inis.iaea.org/records/mpm97-77602/files/4082786.pdf (accessed August 19, 2026).

[4] J.S. Kim, T.S. Jung, J. Yoon, Reactor core design with practical gadolinia burnable absorbers for soluble boron-free operation in the innovative SMR, Nuclear Engineering and Technology 56 (2024) 3144–3154. https://doi.org/10.1016/j.net.2024.03.015.

[5] J.Y. Cho, et al., DeCART2D v1.0 User's Manual, KAERI/TR-5116/2013, Korea Atomic Energy Research Institute, 2013.

[6] J.Y. Cho, et al., MASTER v4.0 User's Manual, KAERI/UM-41/2016, Korea Atomic Energy Research Institute, 2016.

[7] B. T. Rearden, R. A. Lefebvre, and M. A. Jessee, SCALE CODE SYSTEM, ORNL/TM-2005/39 Ver 6.2.4, Oak Ridge National Laboratory, 2020.

[8] J. Leppänen, V. Valtavirta, A. Rintala, R. Tuominen, Status of Serpent Monte Carlo code in 2024, EPJ Nuclear Sci. Technol. 11 (2025) 3. https://doi.org/10.1051/epjn/2024031.

Table II: Whole-core inventories and relative differences with respect to Serpent 2.

at 750 EFPDs (BU=20.06 GWD/MTU)	**Serpent 2 inventory (g)**	**Relative difference with Serpent 2**		
		Single ORIGEN	**Node-wise ORIGEN**	**Pin-wise ORIGEN**
Noble Gases	6.549×10^{4}	-0.53%	0.12%	0.55%
Halogens	2.602×10^{3}	-5.06%	-3.58%	-3.30%
Alkali Metals	3.913×10^{4}	1.99%	1.11%	1.31%
Tellurium Group	6.444×10^{3}	-1.51%	-0.71%	-0.30%
Alkali Earths	2.837×10^{4}	1.82%	0.96%	1.24%
Molybdenum Group	4.848×10^{4}	1.05%	0.79%	1.00%
Noble Metals	4.215×10^{4}	-3.69%	-0.03%	0.40%
Lanthanides	8.890×10^{4}	1.54%	1.54%	1.72%
Cerium Group	2.191×10^{5}	1.97%	0.36%	0.25%
Total	5.407×10^{5}	0.99%	0.59%	0.71%

Table III: Local inventories and relative differences with respect to Serpent 2 for node E7-z16.

at 750 EFPDs (BU=17.3 GWD/MTU)	**Inventory (g)**			**Relative difference with Serpent 2**	
	CR library	**CR-out only**	**Serpent 2**	**CR library**	**CR-out only**
Noble Gases	6.750×10^{1}	6.807×10^{1}	6.827×10^{1}	-1.12%	-0.29%
Halogens	2.828×10^{0}	2.723×10^{0}	2.927×10^{0}	-3.40%	-6.95%
Alkali Metals	4.341×10^{1}	4.262×10^{1}	4.312×10^{1}	0.69%	-1.16%
Tellurium Group	6.861×10^{0}	6.757×10^{0}	6.996×10^{0}	-1.93%	-3.42%
Alkali Earths	3.085×10^{1}	3.127×10^{1}	3.096×10^{1}	-0.36%	1.01%
Molybdenum Group	5.108×10^{1}	5.126×10^{1}	5.139×10^{1}	-0.60%	-0.25%
Noble Metals	4.422×10^{1}	4.220×10^{1}	4.408×10^{1}	0.32%	-4.27%
Lanthanides	9.409×10^{1}	9.459×10^{1}	9.395×10^{1}	0.15%	0.68%
Cerium Group	2.833×10^{2}	2.499×10^{2}	2.796×10^{2}	1.32%	-10.64%
Total	6.242×10^{2}	5.894×10^{2}	6.213×10^{2}	0.46%	-5.14%